

# The phase transformations and structure of $\text{Cu}_{83.34}\text{Pt}_{16.66}$ alloy

HUA CHUN HE, YONG NIAN LI  
*Institute of Precious Metals, Kunming, Yunnan, China*

The structure and phase transformation of  $\text{Cu}_{83.34}\text{Pt}_{16.66}$  alloy have been investigated by X-ray diffraction, TEM, differential thermal analysis, and measurements of electrical resistance and hardness. It was found that this alloy underwent a spinodal order decomposition. During heat treatment, superstructure with an fcc structure was formed rapidly and then progressively transformed to the stable ordered phase  $\text{PtCu}_5$  with an fcr structure.

## 1. Introduction

According to the binary phase diagram compiled by He Chunxiao and Ma Guang-chen [1], the Cu-Pt system forms a continuous solid solution at elevated temperature and shows an order-disorder transformation over a wide range of 3 to 93 at % Cu at low temperature, and a disorder intermittency only as the content of copper reaches 72 at %. Rudniskii [2] reconstructed the Cu-Pt system phase diagram by using the thermoelectric property method. In the copper-rich range (i.e. in the range of 71.39 to 94.61 at %), the forms and transition temperatures of these two phase diagrams are not the same. Pulnickii [2] was the first to discover the intermetallic compound  $\text{PtCu}_5$  from the ultimate value of the dependence of thermoelectric properties on composition, but no study on the structure of the intermetallic compound has so far been reported.

The phase transition and structure of a typical  $\text{PtCu}_5$  alloy (i.e.  $\text{Cu}_{83.34}\text{Pt}_{16.66}$ ) were studied in the present paper by electrical properties, X-ray diffraction and electron microscopy. It was found that the abnormal behaviour of  $\text{Cu}_{83.34}\text{Pt}_{16.66}$  alloy is different from the general order-disorder phase transition, which disagrees with previous results. Therefore it is necessary to make a further investigation.

## 2. Experimental methods

The purities of platinum and copper were 99.98 and 99.999%, respectively. The composition of the alloy was 16.66 at % Pt and the balance copper. The charge was pressed, put into an alumina crucible and then melted in a high-frequency induction furnace in an atmosphere of argon and then cast in a water-cooled copper die-casting. The ingot casting was worked into a thin wire or thin sheet by conventional methods at an intermediate annealing temperature of  $750^\circ\text{C}$  and then water-quenched. The deformation of cold-worked specimens was more than 80%. The quenched material was held at  $750^\circ\text{C}$  for 10 min and then water-quenched. The sample was heat-treated in a protective atmosphere of argon.

The crystal structures of the alloys treated under different heat-treatment conditions were analysed by

using a Geigerflex D/max- $\gamma$ 4 X-ray diffractometer with  $\text{CuK}\alpha$  radiation at 40 kV. The resistance and resistivity of the alloys were measured by conventional methods. The heating rate in the measurement of high-temperature resistance was  $8^\circ\text{Cmin}^{-1}$ . The Vickers hardness of the alloy was measured in an MVK-C hardness tester (load 100 g).

## 3. Results

### 3.1. The relation between resistance and temperature

The relation between resistance and temperature is shown in Fig. 1. The relative resistance change  $\Delta R/R_0$  ( $R_0$  is the resistance at  $0^\circ\text{C}$ ) of the quenched specimen increases with rising measuring temperature, when the temperature is higher than  $250^\circ\text{C}$ , the resistance reduces linearly and reaches a minimum at  $500^\circ\text{C}$ . After that, the resistance increases strongly, then becomes steady when the temperature is higher than  $725^\circ\text{C}$ . The  $(\Delta R/R_0) - T$  curve of the specimen which was aged at  $400^\circ\text{C}$  for 2 h is similar, but the resistance within the range 250 to  $500^\circ\text{C}$  is not reduced so quickly as for the quenched specimen. The room-temperature resistivity was measured after the cold-

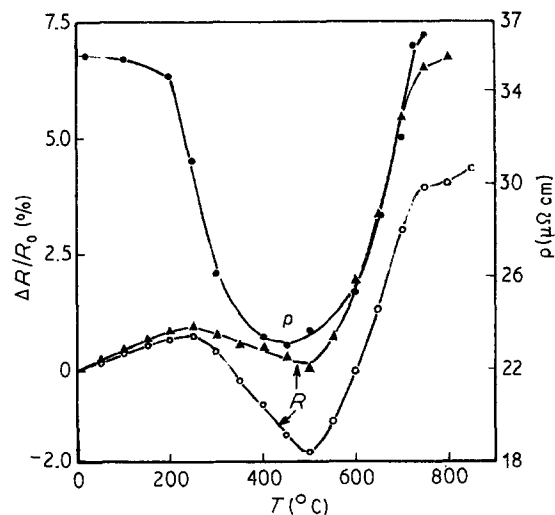


Figure 1 Resistance against temperature: (O) as-quenched; ( $\Delta$ ) as-aged ( $400^\circ\text{C}$ , 2 h); ( $\bullet$ ) as-annealed (10 min).

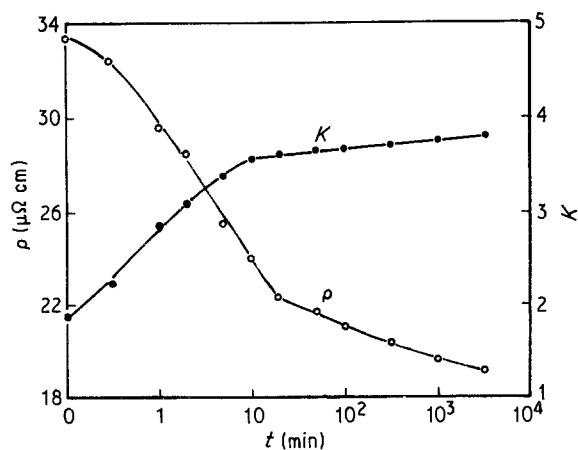


Figure 2 Electrical property changes of cold-worked specimens during ageing at 300°C.

worked specimen was kept at different temperatures for 10 min, and then quenched into water. It can be seen from Fig. 1 that the resistivity varies with quenching temperature in a similar way to the above situation, but its minimum has drifted to 450°C. The difference between cold-worked and annealed resistivity is up to 40%. This indicates that there is an ordering phenomenon in the alloy.

### 3.2. The effect of isothermal ageing on properties

The changes of room-temperature resistivity and strain sensitivity *K* with time of treatment at 300°C for cold-worked specimens are shown in Fig. 2. The resistivity reduces quickly during the first 20 min, while with increase of time the reduction of resistivity becomes slower. However, the change of strain sensitivity with time is just the opposite: it increases quickly at first and then becomes slower after 10 min.

For the quenched specimen aged at 300°C, the relation between hardness and time is illustrated in Fig. 3. The hardness increases with time and reaches a maximum at 300 min; the hardness increase is almost twice as much.

### 3.3. Microstructure of the alloy

The alloy sheet was thinned to about 10 nm using a Model 600 Duai ion mill, then this thin-foil sample was put on a sample holder for observing in a JEM-2000EX electron microscope. It can be seen from Figs 4a, b and c that there exists homogeneously a periodic modulation structure in the whole crystal; this corrugated organization cannot be prevented even with a quenching technique. A periodic composition cluster

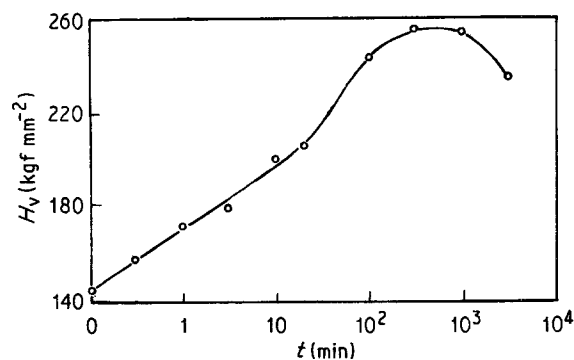


Figure 3 Hardness change of quenched specimens during ageing at 300°C. 1 kgf = 9.8 N.

is shown at the initial stage of ageing, with a modulation wavelength of 8 nm (Fig. 4b). With prolonged time at 400°C (Fig. 4c) the corrugated streak contrast changes from weak to strong and the modulation wavelength increases to 11 nm. The absence of precipitate at grain boundaries and the phase decompositions taking place on both sides of the grain boundaries can be seen from Fig. 4b. These characteristics indicate that spinodal decomposition is produced during the heat-treatment of the alloy. It is seen from the diffraction pattern (Fig. 4d) that there are some ordered diffraction spots in addition to the matrix diffraction spots; this new phase belongs to a tetragonal system by indexing.

### 3.4. Structure analysis

After being kept in the temperature range of 400 to 800°C for 10 min, the alloy was quenched into water at gravity acceleration velocity, then isothermal treatment of the quenched specimen was carried out at 400°C. The crystal structure and changes of the lattice constants of quenched and aged alloys are shown in Fig. 5 and Table I. It can be seen from Fig. 5 that for quenched specimens there are two weak superlattice lines besides the fcc solid-solution lines. With a reduction of quenching temperature or a prolonging of the time at 400°C, the strength of the ordered line increases and the matrix lattice constant gradually reduces. The superstructure formed quickly is unstable and after ageing for 2 h a weak line appears on the left side of (1 1 0). As the time at 400°C increases to 27 h, the new lines become more numerous and stronger, and the superstructure lines disappear. Meanwhile, some new lines become split off from the right-hand sides of (1 1 1), (2 0 0), (2 2 0), (3 1 1) and become more and more clear. The new lines occupy a dominant position after ageing for 100 h. The alloy is transformed to a stable phase PtCu<sub>3</sub> of the tetragonal system.

TABLE I Crystal structure and lattice constants of quenched specimens during ageing at 400°C\*

Property	Time (h)			
	As-quenched	5	50	100
Crystal structure	$\alpha + \alpha'$ (less)	$\alpha + \alpha' + \gamma$ (less)	$\gamma + \alpha$	$\gamma + \alpha$ (less)
Lattice constants (nm)				
<i>a</i>	0.36776	0.36745	0.36720	0.36715
<i>a'</i>			0.308	0.309
<i>c</i>			0.492	0.495

\* $\alpha$  and  $\alpha'$  represent fcc solid solution and superlattice, respectively;  $\gamma$  has the fct tetragonal system with lattice constants *a'* and *c*.

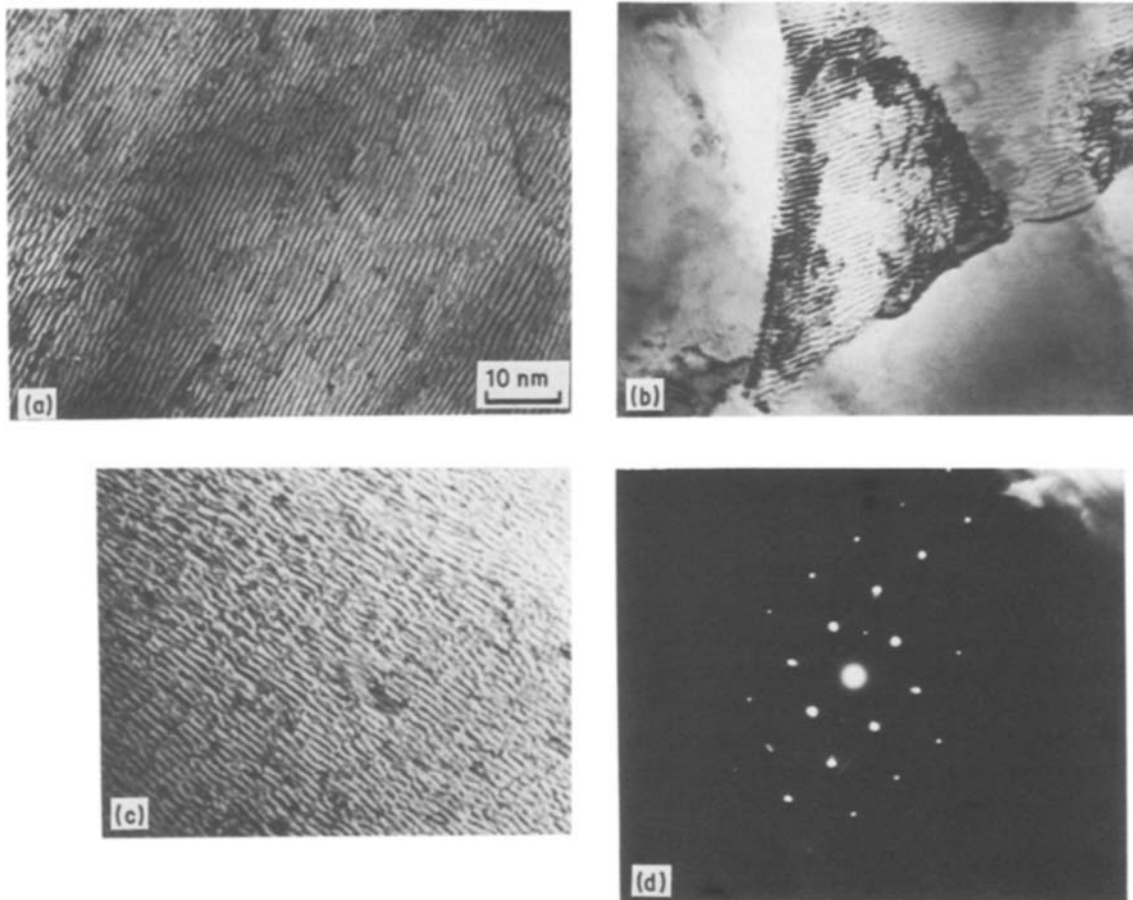


Figure 4 Electron micrographs (a) as-quenched; (b) as cold-worked, 400°C, 10 sec; (c) as-quenched, 400°C, 50 h; (d) diffraction pattern.

### 3.5. Differential thermal analysis (DTA)

The scanning was carried out at the heating rate of  $10^{\circ}\text{C min}^{-1}$  by using a Perkin-Elmer Type 1700 DTA applications. Fig. 6 shows the thermoanalytical curves. The quenched specimen has an exothermic peak at  $334^{\circ}\text{C}$ , but the peak disappears after ageing the specimen at  $400^{\circ}\text{C}$  for 5 h. As the heating rate increases the peak moves toward a higher temperature. The apparent activation energy (1.07 eV) of the exothermic peak can be obtained by using the relation between the heating rate and the peak temperature. There is a consider-

able endothermic peak at  $721^{\circ}\text{C}$  for both quenched and aged specimens. This shows the existence of the first kind of phase transition in  $\text{Cu}_{83.34}\text{Pt}_{16.66}$  alloy.

### 4. Discussion

According to the resistance change and X-ray diffraction pattern at the inception of ageing, the alloy  $\text{Cu}_{83.34}\text{Pt}_{16.66}$  seems to show an ordering phenomenon. However, there exist a series of abnormal behaviours for properties and organization structure, which are different from the general order-disorder phase

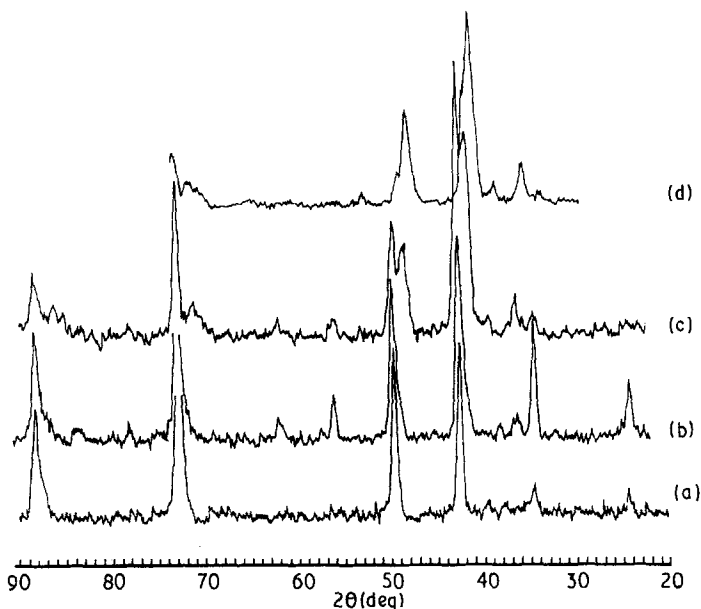


Figure 5 X-ray diffraction patterns of quenched alloys after  $400^{\circ}\text{C}$  heat treatment: (a) 0 h, (b) 2 h, (c) 27 h, (d) 100 h.

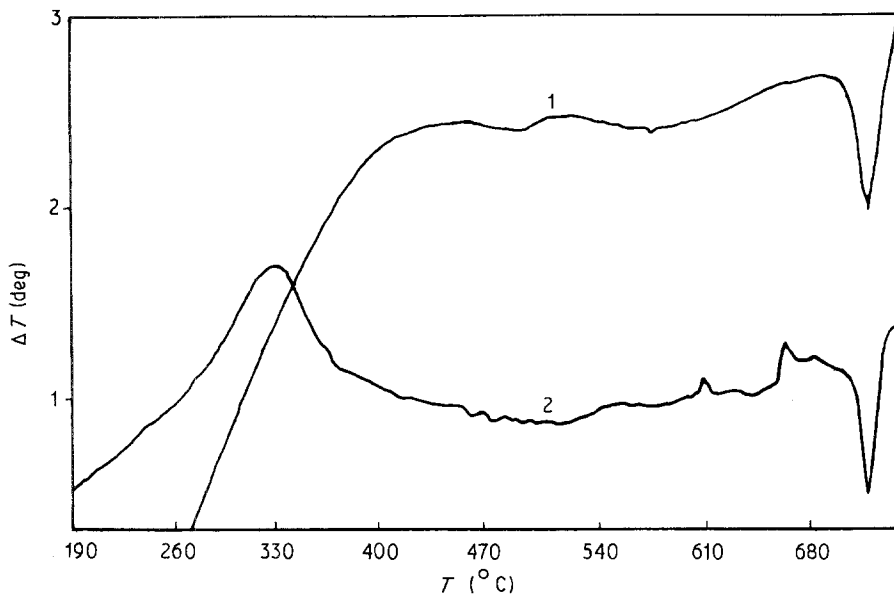


Figure 6 DTA curves: (1) as-aged (400°C, 5 h); (2) as-quenched.

transition. Although it is known that when an alloy transforms from a disordered to an ordered phase, the strain sensitivity should reduce, however the strain sensitivity of the alloy  $\text{Cu}_{83.34}\text{Pt}_{16.66}$  increases as it undergoes an order transformation (see Fig. 2). This behaviour is similar to the precipitation decomposition of supersaturated solid solution. For precipitation decomposition there should be an incubation period at the inception of ageing and then the resistance peak appears, but this is completely at variance with the results shown in Figs 2 and 3. There is no incubation period in the curves of  $\rho$ ,  $K$  and  $H_v$  against  $\log t$ . The resistivity reduces linearly while the value of  $K$  increases linearly; the changes of these properties for this alloy are much greater than for a common ordered alloy. In addition, the transition temperature for an ordered alloy (e.g. AuCu) is a definite point, but for  $\text{Cu}_{83.34}\text{Pt}_{16.66}$  alloy it changes over a wider range of temperature, from disorder at 450°C to complete disorder at 725°C (Fig. 1). Obviously, it is impossible to explain these contradictions only by an order-disorder transformation.

During the initial ageing, a typical periodic modulation structure can be observed even in the quenched state. The corrugated streak contrast becomes stronger with the prolonging of ageing time. This phenomenon cannot be explained by a strain-induced modulation mechanism. Because the modulation structure resulting from a nucleation and growth mechanism appears only at the coarse stage of the last time of ageing, the homogeneous corrugated modulation structure of  $\text{Cu}_{83.34}\text{Pt}_{16.66}$  alloy does not depend on the coarsening process; composition clusters increase gradually without a considerable phase boundary. These characteristics are one of the main pieces of evidence for spinodal decomposition. The process of spinodal decomposition is continuous and homogeneous, and is not very sensitive to defects such as grain boundaries and dislocation, and this is another important characteristic of spinodal decomposition of an alloy. Therefore neither an order-disorder phase transition nor precipitation

decomposition exists in the alloy, and there should exist spinodal order decomposition of the supersaturated solid solution. The temperature of spinodal decomposition is 721°C. The spinodal order decomposition for the alloy, i.e. the coexistence of modulation decomposition and order, is further verified by X-ray analysis. The initial separated products are the fcc ordered phase co-latticed with the matrix. The new phase is in the metastable state and then transforms gradually into the stable ordered phase  $\text{PtCu}_5$  with a tetragonal system with the prolonging of heat treatment. The composition of the alloy  $\text{Cu}_{83.34}\text{Pt}_{16.66}$  is just at the point of tangency of the precipitate and spinodal decomposition curves, and it can be decomposed directly without the process of nucleation and growth. There is no obvious boundary between the decomposed part and the original phase, but a complete co-lattice state. The exothermic peak in Fig. 6 is caused by modulation decomposition. The activation energy of spinodal decomposition is four times smaller than the activation energy of self-diffusion for solute copper.

As it is not necessary to reach the nucleation barrier when the spinodal decomposition takes place, there is no incubation period in the process of decomposition, and the rate of decomposition is very fast, so that the properties and the structures change greatly at the initial ageing stage. Because the separated products are dispersed in the ordered phase, the strengthening effect is obvious: the hardness doubles and redoubles, and the resistivity reduces greatly.

To sum up, the alloy  $\text{Cu}_{83.34}\text{Pt}_{16.66}$  is a disordered solid solution if the temperature is higher than 721°C and undergoes a spinodal order decomposition if the temperature is lower than 721°C. At first a metastable superstructure is formed quickly, then it transforms gradually into the stable ordered phase  $\text{PtCu}_5$  with a tetragonal system. Therefore the conclusions about the solubility curve and the order phase change within the copper-rich range of the Cu-Pt system [1] may be incorrect and should be revised.

### **Acknowledgements**

The authors wish to express their thanks to Tong Li-zhen who attended to the preparation of materials and to Li Shi-lin, Wang Yong-neng, Zhou Yue-hua and Rong Ping who assisted in part of property determinations and structure analysis.

### **References**

1. HE CHUN-XIAO and MA GUANG-CHEN, "Phase Diagrams of Precious Metals Alloys" (1983) p. 73.
2. A. A. RUDNISKII, *Izv. Sectora Fiziko-Khimicheskogo Analiza* **27** (1956) 171.

*Received 3 April*

*and accepted 16 June 1987*